I&EC research
Industrial & Engineering Chemistry Research

Article

pubs.acs.org/IECR

Role of Re and Ru in Re−Ru/C Bimetallic Catalysts for the Aqueous Hydrogenation of Succinic Acid

Xin Di,[†] Chuang Li,[†] Bingsen Zhang,[‡] Ji Qi,[†] Wenzhen Li,[§] Dangsheng Su,[‡] and Changhai Liang*[,†]

[†]Laboratory of Advanced Materials and Catalytic Engineering, School of Chemical Engineering, Dalian University of Technology, Dalian 116024, China

[‡]Shenyang National Laboratory for Materials Science, Institute of Metal Research, Chinese Academy of Sciences, Shenyang 110016, P. R. China

[§]DCBE, Biorenewables Research Laboratory, Iowa State University, Ames, Iowa 50011, United States

Supporting Information

ABSTRACT: To obtain an effective supported metallic catalyst for aqueous hydrogenation of succinic acid (SA), C-supported Re−Ru catalysts with different Re/Ru ratios were sought by using a convenient and environmentally friendly microwave-assisted thermolytic method. The results indicate that the as-prepared Re−Ru/C catalysts exhibit high dispersion with fairly small average particle size (0.7−1.6 nm) and well-structural properties. During the transformation of SA, the Ru composition is responsible for the hydrogenolysis of SA, while the Re composition favors the hydrogenation of SA. The bimetallic Re−Ru interaction promotes the formation of 1,4-butanediol (selectivity is 70.1% with complete conversion), which could rarely be detected when using Re/C or Ru/C monometallic catalysts. The kinetic study further reveals that the introduction of Ru significantly reduces the apparent activation energy from 62 to 40 kJ mol^{-1} and increases the saturation ability of hydrogenation intermediates on the surface of catalysts compared with Re/C. A Re−Ru/C bimetallic catalyst accelerates the formation rate of 1,4-butanediol relative to that of tetrahydrofuran. According to a kinetic mechanism, ring opening of γ-butyrolactone is favored at low temperature, while direct hydrogenation is favored at high temperature.

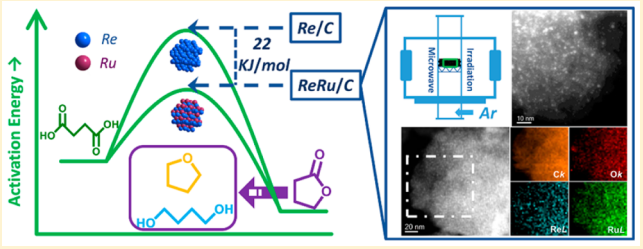

1. INTRODUCTION

According to the data released by the U.S. Department of Energy, succinic acid (SA) belongs to a new class of bioderived building-block chemicals, which can replace the current maleic anhydride C4 platform. The market potential for products based on SA is estimated to be 250000 tons year^{-1}.[1] However, the cost related to purification remains a bottleneck problem for the industrial production of SA from renewable resources,[2] resulting in its lower competitiveness with conversional processes using butane as a raw material. Therefore, research on the direct transformation of SA in an aqueous medium has been going on because it could lower the need for isolating pure SA when using an organic solution as the reaction medium. Furthermore, as an abundant and nontoxic solvent, water is ideal for ionic reaction and provides favorable control of heat during the reaction because of its high enthalpies for phase change and high heat capacity.[3] The petroleum feedstocks usually need to be preprocessed before being used as the raw materials for the production of chemicals.[4] The functionalization step is not required for biomass platform molecules, which can offer numerous synthetic pathways for the production of a wide variety of useful chemicals and thus demonstrates high flexibility. The derivatives of SA such as γ-butyrolactone (GBL), tetrahydrofuran (THF), 1,4-butanediol (BDO), and others[2] are widely used as intermediates and in the synthesis of polymer.[5−7]

Early studies of the aqueous hydrogenation of SA mainly appeared in patent applications, which were merely about theoretical research.[8,9] Recently, many research groups have made great progress on the research of novel catalytic systems, and their work indicated that the activity of the catalysts was highly affected by the metal species.[10−22] Especially, bimetallic catalysts usually exhibit superior catalytic activity because of their synergistic effect.[16−22] For example, the interaction of Ru and Co facilitates the generation of THF,[21] and a higher amount of Re is beneficial for the intermetallic interaction for a Pd−Re/TiO_2 catalyst.[16] However, little systematic investigation was carried on the hydrogenation of SA over supported Re-based bimetallic catalysts, which could effectively reduce both carboxyl and carbonyl compounds.[23] Besides that, the regulating effect of active metals is rarely researched except for some individual work on the influence of the chemical state of Re,[19,22] not to mention the research on the kinetic mechanism of the aqueous hydrogenation of SA. Most of the

Received: December 17, 2016
Revised: April 6, 2017
Accepted: April 7, 2017
Published: April 7, 2017

DOI: 10.1021/acs.iecr.6b04875
Ind. Eng. Chem. Res. 2017, 56, 4672−4683

Table 1. Textural Properties of the Re−Ru/C Bimetallic Catalysts and Times of Flight (TOFs) for the Hydrogenation of SA

catalyst	Re/Ru molar ratio of the bulk phase[a]	Re/Ru molar ratio of the surface phase[a]	average particle diameter (nm)	amount of CO uptake (μmol g_{cat}^{-1})	dispersion (%)[b]	TOFs (h^{-1})[b]
Re/C	1:0	1:0	1.6	48.0	22.3	56
Re3Ru/C	3:1	2.7:1	1.4	57.6	23.7	294
ReRu/C	1:1	1:1	1.1	69.0	24.8	433
ReRu3/C	1:3	1:2.8	0.9	130.9	40.0	275
Ru/C	0:1	0:1	0.7	237.8	60.1	200

[a]The molar ratios of the bulk and surface phases were calculated by ICP-AES and XPS, respectively. [b]Calculated by assuming a stoichiometry factor of CO/metal atom = 1.[23] The TOFs are calculated when the conversion of SA is 20 wt % under 180 °C, 8.0 MPa. The number of active sites used in calculating the TOFs is characterized by CO chemisorption.

researchers have focused their attention on the study of novel supports[12,14,15] and modification of the original catalysts,[10,12,13,16,17] such as the study of the preparation of mesoporous materials and the acid treatment of supports. Considering that novel methods for the preparation of catalysts also remain highly unexplored, there is still a lot of space for further exploration of traditional catalytic components such as Re and Ru for new catalytic performances by modification of the preparation method. Recently, we reported that supported Re/C catalysts were prepared by using a microwave-assisted thermolytic (MAT) method, which is generally more environmentally friendly than conventional wet preparation methods[24] and exhibits good performance for the aqueous hydrogenation of SA to THF. The advantage of this method is the avoidance of using solvents and the use of a favorable heat effect. As a result of the integral and fast feature of microwave heating, this method provides a way to control the textural properties of catalysts and obtainment of highly dispersed catalysts.[25−27]

Herein, we report the synthesis of C-supported Re−Ru catalysts by using the MAT method and evaluate their performance on the aqueous hydrogenation of SA. The influence of active composition on the catalytic activity and the relationship between the textural properties of catalysts and catalysis results will be studied. The catalysts were characterized, and their catalytic performance in the aqueous hydrogenation of SA will be discussed. Meanwhile, the kinetic study is further performed to provide insight into the reaction mechanism, and the regulating effect of active composition from a kinetic perspective will be elucidated.

2. EXPERIMENTAL SECTION

2.1. Catalyst Preparation. Re−Ru/C bimetallic catalysts were prepared with the MAT method using dirhenium decacarbonyl [$Re_2(CO)_{10}$] (99.9%, Acros Organics) and triruthenium dodecacarbonyl [$Ru_3(CO)_{12}$] (98.0%, Acros Organics) as precursors. The coconut-shell-based activated C (surface area, 1400 m^2 g^{-1}; pore volume, 0.7 cm^3 g^{-1}; pore diameter, 1.9 nm), which was pretreated by a HNO_3 solution at 90 °C to remove impurities, was used as supports in this experiment. The mixture of precursors and activated C was mechanically mixed and then transferred to a fluidized quartz tube reactor. The homogeneous mixture was fluidized with Ar to make sure that the reaction mixture was kept under an inert atmosphere and then irradiated by microwave (800 W, 2.45 GHz) for 5 min under an Ar atmosphere in a fluidized state. Then the resultants were cooled to room temperature naturally. The scheme of the MAT method is detailed in the Supporting Information. In our experiments, Re−Ru/C represents all bimetallic catalysts without specifying which one. The Re−Ru catalysts prepared with different Re/Ru atomic ratios (1:0, 3:1, 1:1, 1:3, and 0:1) and the same total metal loading (4 wt %) were identified as Re/C, Re3Ru/C, ReRu/C, ReRu3/C, and Ru/C. In addition, the catalyst containing the same Re loading (2.5 wt %) and higher Ru loading (1.9 wt %) than the ReRu/C catalyst (Re, 2.5 wt %; Ru, 1.5 wt %) was identified as ReRu1.4/C.

2.2. Characterization Method. The actual loading of the Re−Ru/C bimetallic catalysts was analyzed by inductively coupled plasma atomic emission spectroscopy (ICP-AES). The amount of active sites and the dispersion of Re−Ru/C catalysts were measured with CO chemisorption. The amount of irreversibly adsorbed CO was determined as the extrapolation of the difference between the total uptake and the reversible uptake to zero pressure. X-ray diffraction (XRD), H-assisted temperature-programmed reduction (H_2-TPR), transmission electron microscopy (TEM), scanning transmission electron microscopy (STEM), and corresponding elemental mapping were performed to investigate the structure properties and metallic interaction. The catalyst samples were prereduced by H_2 under 300 °C for 120 min before measurement of TEM and STEM. H_2-TPD was carried out to study the ability of H_2 adsorption and activation of Re−Ru/C bimetallic catalysts. The surface composition and chemical state of the catalysts were researched by X-ray photoelectron spectroscopy (XPS). Before measurement, the samples were stored under the same conditions and it was ensured that they were exposed to the air for the same period of time. After that, these samples were analyzed by XPS simultaneously to reduce the experimental error to the maximum extent. The more specific information is listed in the Supporting Information.

2.3. Catalyst Evaluation. The aqueous hydrogenation of SA was carried out in a 50 mL autoclave (Hastelloy alloy) with a magnetic stirrer and a temperature controller unit. The catalysts were pretreated in a flow of H_2 at 300 °C for 120 min before reaction. After that, the catalysts were transferred to a batch autoclave under the protection of an Ar atmosphere as soon as possible, and then it was protected by water solutions of SA. After several minutes, the batch autoclave was purged with H_2 three times to remove air. The reactor was heated to the desired temperature and purged with H_2 to the desired pressure at that time. The reaction was performed under constant pressure by using a pressure control system and with continuous stirring to remove the influence of external diffusion. After the reaction, the reactor was cooled to room temperature with water and H_2 was released. The spent catalysts were filtered, washed, and dried before collection. The uncertainties of the temperature, pressure, and stirring speed were ±0.1 °C, ±0.05 MPa, and ±1 rpm min^{-1}.

The conversion of SA was analyzed by a liquid chromatograph (Waters 1525, USA), equipped with an ultraviolet detector and a C18 column (Welch, Ultimate LP-C18, China). An aqueous phosphoric acid solution (5 mM) was used as the mobile phase, and the absorbed wavelength was 204 nm. The selectivity of the reaction product was analyzed by a gas chromatograph (Tianmei GC7890, China) equipped with a FFAP capillary column. Isopropyl alcohol was used as the internal standard. Products were also identified using a gas chromatograph−mass spectrometer (Agilent 7000B, USA) and a liquid chromatograph−mass spectrometer (Thermo Scientific TSQ Quantum Ultra, USA). The possible presence of Re or Ru in solution was investigated by ICP-AES equipment.

The conversion and selectivity were calculated as follows:

$$\text{conversion } (X_{SA}) = \frac{n_0 - n_t}{n_0}$$

DOI: 10.1021/acs.iecr.6b04875
Ind. Eng. Chem. Res. 2017, 56, 4672−4683

$$\text{selectivity } (S_i) = \frac{m_i}{\sum m_i}$$

where n_0 represents the initial molar quantity of SA, n_t represents the molar quantity of SA at time t, and m_i represents the molar quantity of product i. The C balance is kept above 96% in all of the experiments.

3. RESULTS AND DISCUSSION

3.1. Characterization of Re−Ru/C Bimetallic Catalysts.

As seen in Table 1, the actual molar ratio is similar to the theoretical ratio whether in the bulk or surface phase. Only a low degree of elemental segregation, which is common in bimetallic catalysts, was detected on the surface of the Re3Ru/C and ReRu3/C catalysts. The integral and fast feature of microwave heating contributes to the decreased atomic migration, which was often caused by the common heating progress. From the XRD patterns in Figure S1, no discernible characteristic diffraction peaks corresponding to Re or Ru are observed in the samples but are observed for the diffraction peaks of activated C, indicating that the metallic particles are too small to be resolved (less than 4 nm) by XRD.

To further study the structural and compositional distribution, TEM was carried out. The TEM images in Figure 1 confirm that the metal particles are well dispersed on the surface of a C support and exhibit nonsymmetrical shapes with average particle diameters ranging from 0.7 to 1.6 nm. It is worth noting that the average particle diameter decreases sharply with increasing molar ratio of Ru. As shown in Table 1, the amount of CO uptake and dispersion for the Re−Ru/C bimetallic catalysts significantly increased with a decrease in the particle size, which is caused by a small particle effect. This result is different from some other research that Re contributes to the dispersion of Re−Ru bimetallic catalysts.[28] In our experiments, the Ru particle size of Ru/C is less than that of Re/C and the Ru element contributes to the decrease of the particle size for bimetallic catalyst prepared with the MAT method, which is different from the catalyst prepared with the incipient wetness impregnation method in this Article.[28] The aggregation of atoms and particles during the preparation process may be inhibited when using carbonyl compounds as precursors, which can be rapidly decomposed into zerovalent atoms under microwave heating. This comparison further confirms the effect of small particle size in our experiments. The ReRu/C sample was further characterized by high-angle annular dark-field STEM (HAADF-STEM) images and the corresponding elemental maps shown in Figure 2. It exhibits a homogeneous distribution of Re, Ru, and ReRu/C samples. The existence of O is due to the O-containing groups on activated C obtained from its pretreating process by a nitric acid solution. According to elemental mappings, there is interaction between Re and Ru, and these elements did not exist in isolation. Meanwhile, the HAADF-STEM and elemental maps also further demonstrate the fairly small particle size and well dispersion of Re and Ru particles on the ReRu/C catalyst.

TPR experiments were carried out with a H_2/Ar gas mixture to further investigate the phase state and Re−Ru interaction of bimetallic catalysts, and the results are shown in Figure 3. The peaks detected at 375 and 130 °C for Re/C and Ru/C monometallic catalysts, respectively, are assigned to the reduction of rhenium or ruthenium oxides, which are caused by the reoxidation of metal after exposure to air.[29,30] It is known that Re is easily oxidized and reduced with difficulty compared with Ru. This phenomenon manifests as higher reduction temperatures for Re/C catalysts than for Ru/C

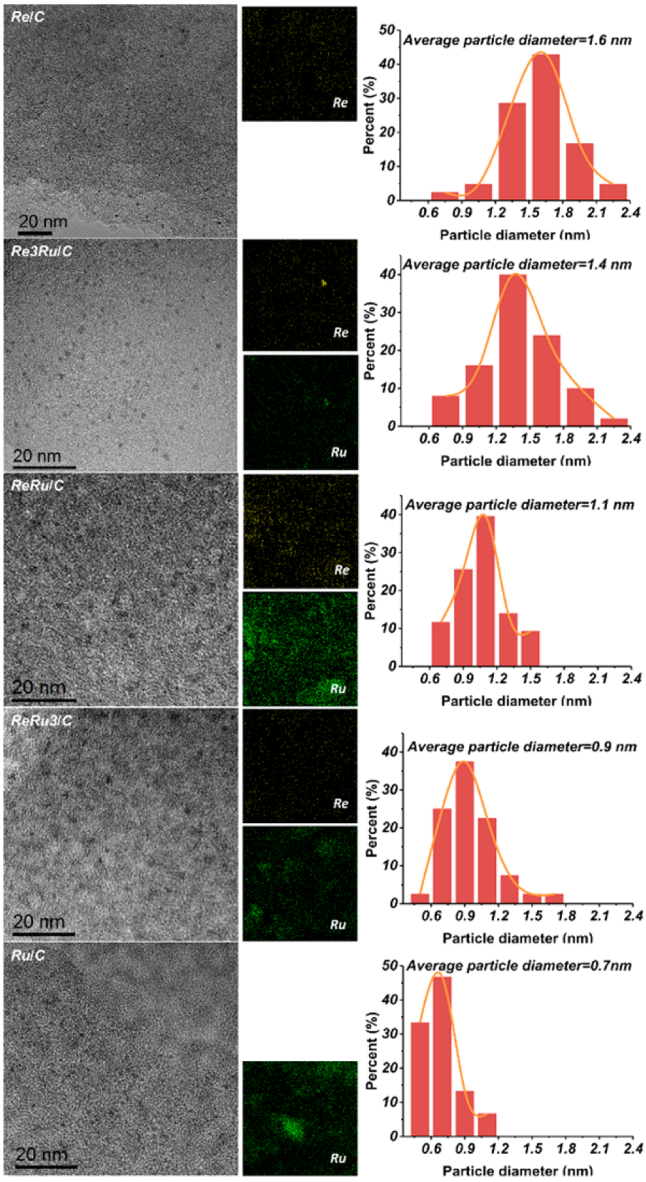

Figure 1. TEM images and SEM elemental mappings of Re−Ru/C bimetallic catalysts that are prereduced by H_2.

catalysts. The primary reduction temperature for bimetallic catalysts was between that of two monometallic catalysts, and the increase of the Re molar ratio resulted in the growth of the reduction temperature. The reduction of metallic oxides at this primary reduction temperature can be attributed to the coreduction of Re and Ru for bimetallic catalysts. This indicates that Re is alloyed or in close interaction with the Ru metal, which can also be identified by the TEM elemental mapping. The promotion of the Re reduction can be attributed to the H_2 spillover from the previously reduced Ru to Re species.[31] The H_2 consumption of all samples at high temperature (500−700 °C) was attributed to methane formation coming from the reduction of functionalized C on the catalyst support. For these samples, the supports were pretreated with a nitric acid solution before the preparation of catalysts. Because of that, a part of C on the surface easily reacts with H_2. Meanwhile, the reduced metal also contributes to the formation of methane under a H_2/Ar atmosphere.[31] The primary consumption temperature of H_2 decreased from 635 to 585 °C with increasing Ru amount,

DOI: 10.1021/acs.iecr.6b04875
Ind. Eng. Chem. Res. 2017, 56, 4672−4683

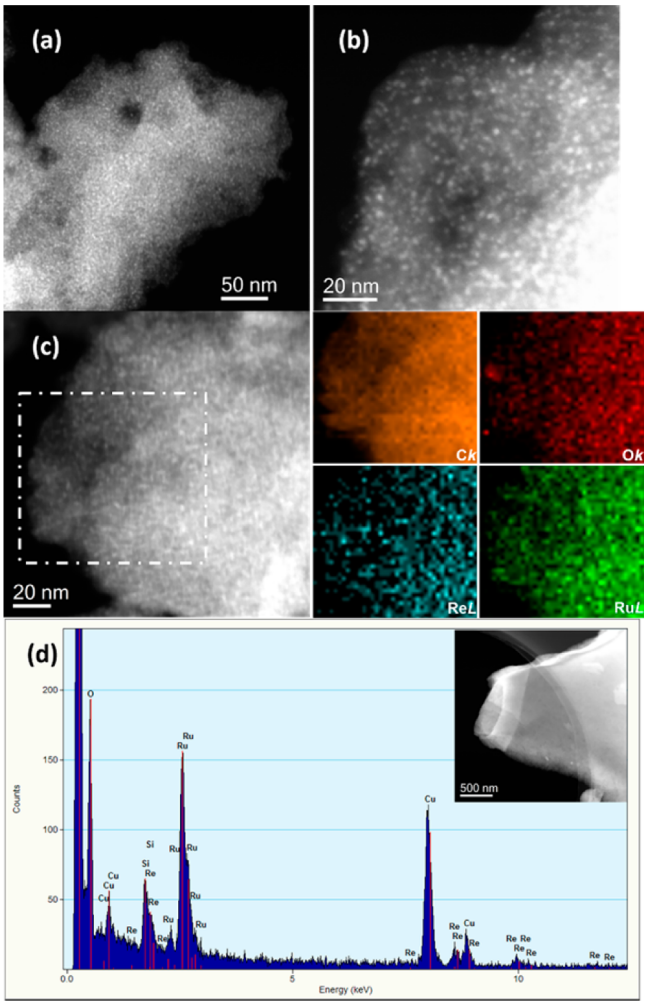

Figure 2. HAADF-STEM images (a and b), elemental mappings (c), and energy-dispersive X-ray results (d) of ReRu/C catalysts.

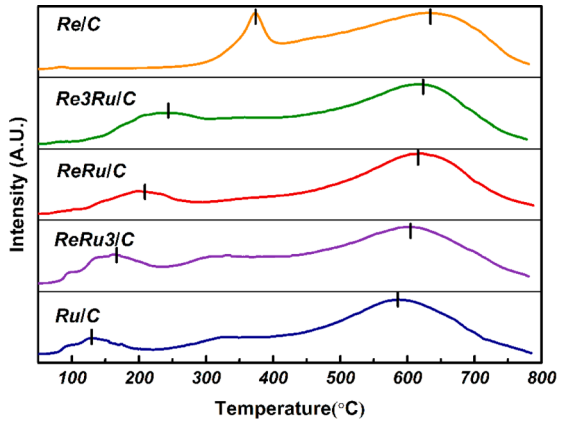

Figure 3. TPR profiles of Re−Ru/C bimetallic catalysts.

showing that Ru is more advantageous to the formation of methane compared with Re.

XPS was utilized to determine the surface composition, chemical state, and interaction between Re and Ru of the catalysts. A typical wide energy scan of the bimetallic catalysts gave an XPS spectrum with clearly resolved C 1s, O 1s, Ru 3p, Ru 3d, Re 4f, and Re 4d peaks. The Re 4f peak was used for quantitative measurements of Re, and the Ru 3p peak was applied to quantitative analysis considering that Ru 3d is almost coincident with C 1s. According to the spin−orbit, the Re 4f and Ru 3p peaks can be deconvoluted into Re $4f_{7/2}$ and Re $4f_{5/2}$ and into Ru $3p_{3/2}$ and Ru $3p_{1/2}$, which have shifts of 2.4 and 4.1 eV respectively. The distribution of Re and Ru chemical states in the catalysts that were oxidized by air was estimated by the curve fit of Re 4f and Ru 3p, as presented in Figure 4. The deconvoluted peaks at 40.7, 42.3, and 45.1 eV in Figure 4 (left) are assigned to Re $4f_{7/2}$ lines and confirm the existence of Re^0, Re^{4+}, and Re^{6+} species, respectively.[18,32,33] On the other hand, the Ru 3p peak could be divided into Ru^0 (462.4 eV) and Ru^{4+} (464.7 eV) species.[18,34] Although the XPS measurements were not carried out under in situ conditions, the characterization results can afford much useful information for the structure properties of the catalysts. As shown in Figure 4, a position shift (0.2−0.4 eV) in the binding energy can be observed for Re−Ru/C bimetallic catalysts with respect to Re/C monometallic catalysts, indicating the existence of interaction between Ru and Re, which can be also certified by the binding energy shift of Ru. On the basis of peak areas obtained by curve-fitting results, the oxidation state ratio was quantified, as summarized in Table S1. For all catalysts, the ratio of high-valent rhenium oxide was above 60%; however, zerovalent Ru exhibits a ratio similar to that of ruthenium oxide. It demonstrates that Re exists primarily in the oxidation state, and Ru is difficult to oxidize when exposed to air compared with Re. Moreover, the ReRu/C catalyst exhibits a much higher proportion of zerovalent Re than other bimetallic catalysts, which shows that the Re−Ru interaction exists in the ReRu/C catalyst and contributes to the stability of metallic Re. XPS and H_2-TPR results reveal that the interaction between Re and Ru not only is beneficial to the reduction of rhenium oxide caused by H_2 spillover but also contributes to the stability of metallic Re when exposed to air.

The catalytic activity of supported catalysts usually relies largely on the amount of adsorbed H_2 on surface active sites. Thus, H_2-TPD measurements were carried out to study the ability of adsorbing H_2 and the character of active sites for Re−Ru bimetallic catalysts. Thermal desorption curves of H_2 from the various samples are presented in Figure 5. The profiles of all samples show a small broad peak in the temperature range of 100−280 °C, which can be attributed to the reversible adsorption of H_2 on the surface of catalysts. A broad peak ranging from 300 to 600 °C is detected in all samples even on the support. For the C support, the broad peak could correspond to the reduction of functionalized C on the surface caused by H_2 spillover according to the results in H_2-TPR. In our opinion, the broad peak existing in Re−Ru/C bimetallic catalysts is caused by the dissociation of adsorbed H_2 and methanation of the support. However, this phenomenon significantly relies on the adsorbed H, and methanation of the pure support is really small compared with dissociation of H_2 on Re−Ru/C bimetallic catalysts (Figure 5). Because of that, it is reasonable to investigate the ability of activating H_2 by the peak ranging from 300 to 600 °C. The peak was divided into three regions (peaks I−III) by simulation, and these three peaks represent the different relatively adsorption degrees of H_2 according to the dissociative temperature (peak I was identified as weak adsorption, peak II as medium adsorption, and peak III as strong adsorption). The peak area of peak I on Re/C catalysts was used as the standard for quantitative analysis, and the amount of relative H_2 dissociation was calculated according to the following equation:

DOI: 10.1021/acs.iecr.6b04875
Ind. Eng. Chem. Res. 2017, 56, 4672−4683

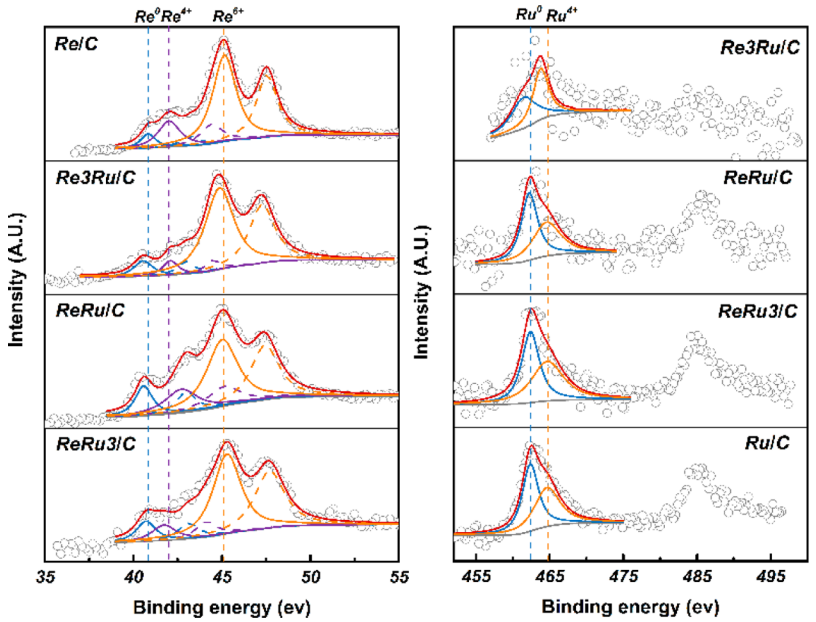

Figure 4. Results of XPS for Re 4f and Ru 3p: gray circles, raw data; blue line, $4f_{7/2}$ and $4f_{5/2}$ for Re^0 and $3p_{3/2}$ and $3p_{1/2}$ for Ru^0; violet line, $4f_{7/2}$ and $4f_{5/2}$ for Re^{4+}; orange line, $4f_{7/2}$ and $4f_{5/2}$ for Re^{6+} and $3p_{3/2}$ and $3p_{1/2}$ for Ru^{4+}; red line: the result of fitting.

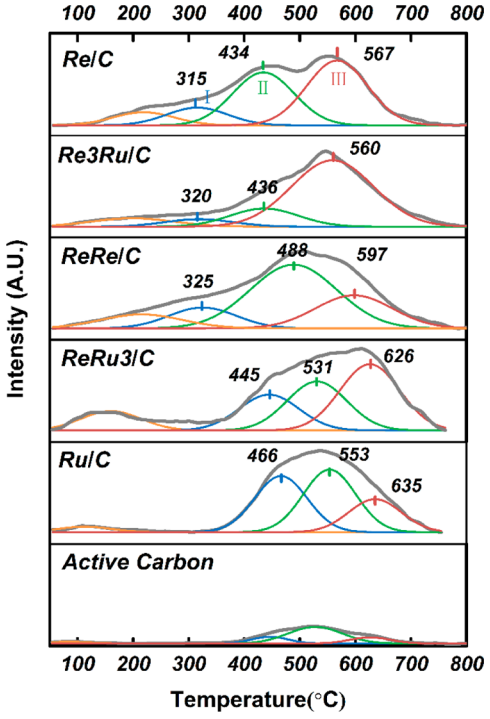

Figure 5. Results of H_2-TPD for Re−Ru/C bimetallic catalysts.

$$\text{amount of relative } H_2 \text{ dissociation} = \frac{\text{peak area of the Re−Ru/C catalyst}}{\text{metal content of Re−Ru/C (mol)}} \div \frac{\text{peak area of peak I on the Re−Ru/C catalyst}}{\text{metal content of Re/C (mol)}}$$

The amount of relative H_2 dissociation is listed in Table S2. The amount of relative H_2 dissociation gradually increased from 7.7 to 9.2 with an increase of the molar ratio of Ru under the same metal loading, and the ReRu/C catalyst exhibited a higher amount of relative H_2 dissociation (9.0) than Re3Ru/C (8.5) and ReRu3/C (8.9) catalysts. As a result, it is concluded that Ru is in favor of the adsorption of H_2 compared with Re components, and the Re−Ru interaction on the Re−Ru/C catalyst further enhances the ability of an activating H_2 molecule. For the Re/C catalyst, the main dissociative temperatures for weak, medium, and strong adsorption are 315, 434, and 567 °C, but for the Ru/C catalyst, the main dissociative temperatures are 466, 553, and 635 °C. An increase in the molar ratio of Ru leads to an increase in the dissociative temperature, as shown in Figure 5. Because of the strong H_2 adsorption ability of Ru, the adsorbed H_2 is not easily dissociated from the surface of metallic active sites after adsorption and thus shows a higher dissociative temperature. Besides, by the influence of intermetallic interaction, medium adsorption of H_2 takes the dominant place for the ReRu/C (5.3) catalyst, which is different from the Re3Ru/C (1.4) and ReRu3/C (2.9) catalysts. Thus, it can be seen that the Re−Ru interaction on the ReRu/C catalyst not only strengthens the H_2 activation and adsorption but also contributes to the H_2 adsorption of Re−Ru metallic active sites.

3.2. Aqueous Hydrogenation of SA. The activity of different catalysts in the aqueous hydrogenation of SA is shown in Figure 6. The increase of the Ru atomic ratio led to a significant increase in the conversion of SA. To understand this activity more, the turnover frequencies (TOFs) were calculated in this experiment according to CO chemical adsorption, as shown in Table 1. The Re−Ru bimetallic catalysts showed higher TOF values than the monometallic catalysts. The TOF values first increased and then decreased with increasing Ru atomic ratio. The ReRu/C catalyst exhibited higher TOFs (433 h^{-1}) than other catalysts such as Re/C (56 h^{-1}) and Ru/C (200 h^{-1}) monometallic catalysts. It can be seen that the introduction of Ru improves the activity efficaciously. From our perspective, this result is closely related to the average particle sizes. On the basis of TEM images, the average particle diameter decreases sharply from 1.6 to 0.7 nm with an increase of the molar ratio of Ru. A decrease of the particle size results in

DOI: 10.1021/acs.iecr.6b04875
Ind. Eng. Chem. Res. 2017, 56, 4672−4683

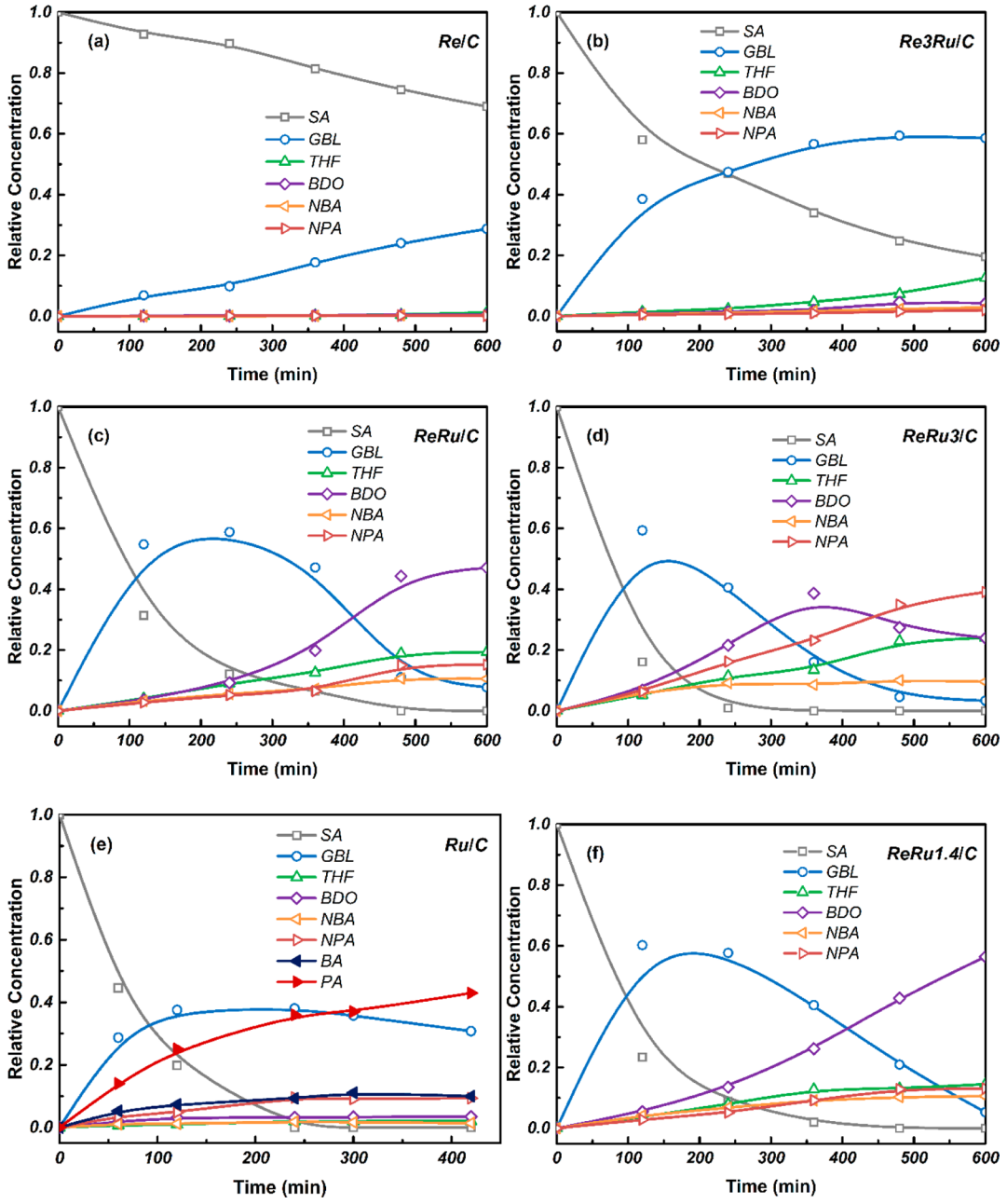

Figure 6. Product distribution for the aqueous hydrogenation of SA over Re−Ru/C bimetallic catalysts. Reaction conditions: 180 °C, 8.0 MPa, 20 g of solutions (10 wt % SA), 0.2 g of catalysts.

a significant increase of active sites according to CO chemical adsorption, which contribute to an increase of the catalytic activity. Besides, the interaction between Re and Ru also plays a key role in the transformation of SA considering the fact that higher TOFs are observed on ReRu/C instead of Ru/C, which has minimum average particle size. Re^0 nanoparticles are easily oxidized to ReO_X species when exposed to air as a result of the weak interaction between the metal and support.[19] The interaction between Re and Ru is beneficial to the stabilization of Re^0 by strengthening the interaction between the metal and support, which can be validated by the XPS results that ReRu/C showing the strongest interaction has a higher Re^0 proportion. As a result, this strong Re−Ru interaction of ReRu/C is beneficial to the hydrogenation of SA to GBL, leading to the maximum TOFs achieved on it.

From the results of the product distribution in Figure 6a and our previous work, over the Re/C monometallic catalyst, the hydrogenation of SA was a consecutive reaction and the final product was THF, which was generated from the further hydrogenation of intermediate product GBL. Different from the Re/C catalyst, the Ru/C monometallic catalyst did not show the character of the consecutive reaction, as shown in Figure 6e. PA and GBL were major components in the products, and PA mainly came from the hydrogenolysis of SA. It can be found that the Ru composition contributes to the hydrogenolysis of SA rather than the hydrogenation, which is different from the Re composition. The hydrogenolysis properties of Ru may be related to its nature, and some researchers have reported that Ru is beneficial to the breakage of the C−C bond.[35,36] Furthermore, compared with some other works in which the

DOI: 10.1021/acs.iecr.6b04875
Ind. Eng. Chem. Res. 2017, 56, 4672−4683

hydrogenolysis properties were not significant,[13,18,21] we hold the opinion that the small particle size of Ru also strengthens this nature. In this work, the average particle size of Ru/C is relatively larger than that in our other experiments. Because of that, the hydrogenolysis properties of Ru will be suppressed by the large particle size. H_2-TPD data imply that H_2 is strongly adsorbed on the Ru/C catalyst compared with other catalysts. We hold the opinion that the strongly adsorbed H_2 contributes to breakage of the C−C bond on a portion of the R−CH_2−COOH group in SA, instead of hydrogenation of −C═O on the R−CH_2−COOH group. The introduction of Re improves the hydrogenation performance of the Re−Ru bimetallic catalyst, so as to reduce the hydrogenolysis of SA. There is sufficient evidence that PA is barely detected on Re3Ru/C, ReRu/C, and ReRu3/C catalysts. The proposed reaction mechanism for SA hydrogenation over Ru/C and ReRu/C is shown in Schemes S2 and S3. What is of interest is that NPA more or less increases in the product distribution for all Re−Ru/C bimetallic catalysts, and this phenomenon can be due to two reasons. First, Re−Ru/C bimetallic catalysts accelerate the hydrogenolysis of BDO to NPA compared with the Re monometallic catalyst, in spite of the fact that they could reduce the direct hydrogenolysis of SA to PA by the addition of Re. Furthermore, PA will be quickly hydrogenated to NPA because of the introduction Re, which barely happens on the Ru/C catalyst according to the data in Table S3.

Over Re−Ru/C bimetallic catalysts (Re3Ru/C, ReRu/C, and ReRu3/C), the hydrogenation of SA was a consecutive reaction and BDO was the main product, which is significantly different from Re/C and Ru/C monometallic catalysts. The ReRu/C catalyst exhibits higher selectivity to BDO than ReRu3/C and ReRu3/C catalysts. As a consequence, we infer that the Re−Ru interaction contributes to the generation of BDO especially for ReRu/C, which shows the strongest intermetallic interaction according to XPS. The introduction of Re reduced the hydrogenolysis performance, and the Re−Ru interaction influenced the adsorption of active components on the surface of ReRu/C catalysts, thereby favoring ring opening of GBL by hydrogenation to BDO instead of dehydration by hydrogenation to THF, as shown in Scheme S3. This kinetic study further proved that Re−Ru interaction relatively increases the generation rate of BDO over THF. On the basis of Figure 6f, the selectivity to BDO can benefit from the moderate increase of the Ru ratio, which can strengthen the Re−Ru interaction; for instance, the selectivity to BDO on the ReRu1.4/C catalyst is 10% higher than that on the ReRu/C catalyst. However, a further increase in the ratio of Ru such as ReRu3/C contributes to the hydrogenolysis and dehydration of BDO to NPA and THF, respectively, in turn suppressing the generation of BDO. Moreover, we hold the opinion that the medium H_2 adsorption sites can also provide more favorable active sites for the generation of BDO over Re−Ru/C bimetallic catalysts considering that the selectivity to BDO increases in the order of Re3Ru/C < ReRu3/C < ReRu/C, which is consistent with the relative amount of medium H_2 adsorption (peak II in H_2-TPD), as shown in Table S2. Some other works also proved the opinion in this experiment that the medium H_2 adsorption could increase the catalytic activity of the generated diols.[18] The generation of BDO was favored by not only the H_2 adsorption behavior but also the Re−Ru interaction.

The transformation of an intermediate product was also studied in this work, and the results are consistent with the conclusions above. It was found that the main products were THF and BDO when using GBL as the reactant over ReRu/C and Re/C catalysts; however, less BDO or THF was detected, and the main product was PA over the Ru/C catalyst, as shown in Table S3. This indicates that Ru contributes to hydrogenolysis and Re favors hydrogenation, which has already been proven above. From the results, the main product was THF and less NPA was detected on the Re/C catalyst when using BDO as the reactant, compared to the high amount of NPA detected on Ru/C and ReRu/C catalysts. Furthermore, the Re/C catalysts could transfer BA and PA to NBA and NPA, respectively, by hydrogenation, which is more effective on the ReRu/C catalyst. However, over the Ru/C catalyst, BA and PA were hardly hydrogenated to NBA and NPA. This also explains the larger amount of NPA in the liquid product over the ReRu/C catalyst. As a result of the introduction of Ru, the ReRu/C catalyst promotes the hydrogenolysis of BDO, so that the selectivity to NPA is higher than that of the Re/C catalyst. In addition, the highly efficient hydrogenation of PA on the ReRu/C catalyst also results in an increase of NPA to a certain extent. In summary, the research on the transformation of an intermediate product further confirms the conclusions above, and the main reaction pathway is shown in Scheme 1.

Scheme 1. Main Reactive Route for the Catalytic Hydrogenation of SA

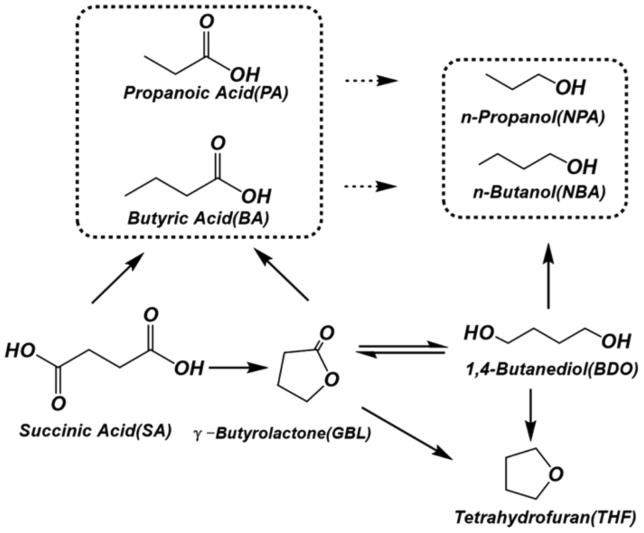

3.3. Kinetic Study. *3.3.1. Kinetic Study on the Hydrogenation of SA.* Analysis of the kinetics is essential to sufficiently explain the interaction between the structural properties and catalytic activity. However, only a few researches about this study were reported to our best knowledge and not to mention analysis of the catalytic activities. We performed a kinetic study of the main reaction pathway, as shown in Scheme 2. Details for each experiment are provided in the following subsections. In this experiment, the influence of external and internal transport was eliminated as far as possible by controlling the reaction conditions (Supporting Information).

The hydrogenation of SA to GBL (step 1) was first researched, and the reaction conditions (temperature, pressure, concentration, reaction time, etc.) were controlled to make sure that the major SA hydrogenated product was GBL (>90% selectivity). In this experiment, details about the fitting method and process are listed in the Supporting Information. The fitting results reveal that the apparent reaction orders for the

DOI: 10.1021/acs.iecr.6b04875
Ind. Eng. Chem. Res. 2017, 56, 4672−4683

Scheme 2. Main Reaction Pathway for the Kinetic Study

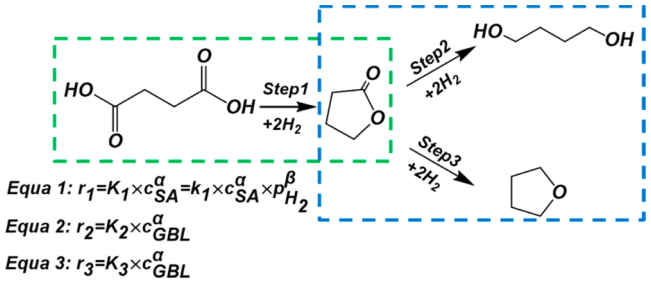

concentration of SA are 0.6 over the ReRu/C catalyst and 1.0 over the Re/C catalyst with a range of SA concentrations (0.5−0.85 M). This observation is consistent with a previous study in which apparent reaction orders between 0 and 1 are generally observed for hydrogenation of the C═O bond over noble metals. Rachmady and Vannice reported that the apparent reaction orders are 0.2−0.4 for the hydrogenation of acetic acid over Pt/TiO_2.[37] Apparent reaction orders of 0.1 and 0.8 were observed over $Pd–Re/SiO_2$ and Re/SiO_2 catalysts, respectively, for the hydrogenation of stearic acid.[33] Bond et al. have reported that the apparent reaction orders are 0 for the hydrogenation of levulinic acid and 1 for the hydrogenation of 4-hydroxypentanoic acid over the Ru/C catalyst.[38] For the hydrogenation of arabinonic acid, an apparent reaction order of 0 was also observed over the Ru/C catalyst.[39] To the best of our knowledge, the apparent reaction order of 0.6 for hydrogenation is typically attributed to the hydrogenation intermediates that incompletely saturate the available metal surface sites, which is different from the zero-order reaction.[38] The saturability of the hydrogenation intermediates on Re−Ru/C are higher than those on the Re/C catalyst, which means that the ReRu/C catalyst is more beneficial to the adsorption activation of active components. The Re/C monometallic catalyst will be more influenced by the SA concentration than the ReRu/C bimetallic catalyst as the reaction progresses. Figure 7C illustrates the dependence of the reaction rate constants (K_1) on the H_2 pressure, and the regression of data reveals an apparent reaction order of 1.9 over ReRu/C. The rate of carboxyl group hydrogenation is often apparently influenced by the H_2 pressure. This phenomenon is also proven by our work that SA hydrogenation usually needs fairly high H_2 pressure. Tomishige et al. observed an apparent reaction order of 1.2 for H_2 pressure in the hydrogenation of stearic acid over the $Pd–Re/SiO_2$ catalyst.[33] A reaction order of 0.6 was found for the hydrogenation of LA by Bond et al. over the Ru/C catalyst. Similarly, half-order H_2 dependencies were observed by Rachmady and Vannice in acetic acid hydrogenation over a supported Pt catalyst.[37] Our research shows that the hydrogenation of SA over ReRu/C is well represented by the following empirical rate law:

$$r_{SA} = K_1 c_{SA}^{0.6} = k_1 c_{SA}^{0.6} p_{H_2}^{1.9}$$

The concentration of SA in an aqueous solution was found to have a limited effect on the catalytic activity of hydrogenation compared with the H_2 pressure. The results suggest that the hydrogenation of SA is sensitive to the H_2 pressure and the dissociation of H_2 or the reaction of the dissociated H_2 species is involved in the rate-determining step. Considering the fast dissociation of H_2 over Re-based catalysts, the reaction of the dissociated H_2 species will be the rate-determining step.[33]

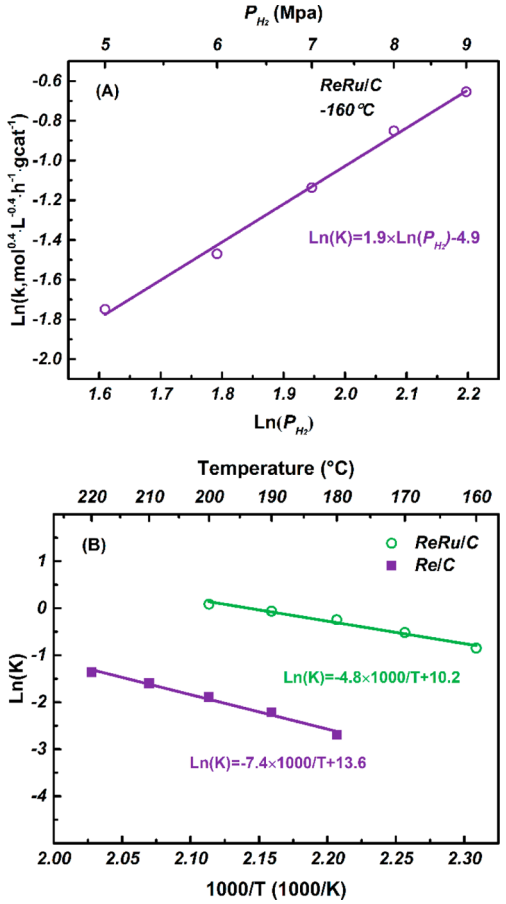

Figure 7. (A) Dependence of the reaction rate constants (K_1) on the H_2 pressure over Re−Ru/C catalysts (the correlation coefficient R^2 > 0.99) and (B) Arrhenius plots for the hydrogenation of SA to GBL over Re−Ru/C and Re/C catalysts (the correlation coefficient R^2 > 0.98).

In Figure 7B,C, Arrhenius plots for the Re/C and ReRu/C catalysts are provided, and the fitting data are summarized in Table 2. For this set of catalysts, the addition of Ru increased the hydrogenation activity approximately 7−10-fold at temperatures of 160−220 °C, according to the apparent reaction rate constants (K_1) in Table 2 even though the influence of the SA concentration was considered. From the kinetics perspective, this phenomenon can be attributed to the influence of the active sites and apparent activation energy. The CO chemisorb and TEM images showed that the ReRu/C catalyst possessed more active sites than the Re/C catalyst as a result of the

Table 2. Reaction Rate Constants (K_1) and Apparent Activation Energies for the Hydrogenation of SA over Re/C and ReRu/C Catalysts under 8.0 MPa

	Re/C (h^{-1} g_{cat}^{-1})	ReRu/C ($mol^{0.4}$ $L^{-0.4}$ h^{-1} g_{cat}^{-1})
160 °C		0.43 ± 0.014
170 °C		0.60 ± 0.015
180 °C	0.07 ± 0.001	0.78 ± 0.015
190 °C	0.11 ± 0.003	0.94 ± 0.010
200 °C	0.15 ± 0.004	1.09 ± 0.013
210 °C	0.20 ± 0.005	
220 °C	0.26 ± 0.006	
E (kJ/mol)	62 ± 4	40 ± 3

DOI: 10.1021/acs.iecr.6b04875
Ind. Eng. Chem. Res. 2017, 56, 4672−4683

Table 3. Reaction Rate Constants (K) and Apparent Activation Energies for the Hydrogenation of GBL over Re/C and ReRu/C Catalysts under 8.0 MPa

	ReRu/C				Re/C			
	K_{BDO} (mol L^{-1} h^{-1} g^{-1})	K_{THF} (h^{-1} g^{-1})	K_{BDO}/K_{THF}	r_{BDO}/r_{THF}[a]	K_{BDO} (mol L^{-1} h^{-1} g^{-1})	K_{THF} (h^{-1} g^{-1})	K_{BDO}/K_{THF}	r_{BDO}/r_{THF}[a]
140 °C	2.5×10^{-1}	6.8×10^{-3}	36.4	31.4	1.0×10^{-2}	5.9×10^{-4}	17.0	14.6
150 °C	2.8×10^{-1}	1.4×10^{-2}	20.5	17.7	1.2×10^{-2}	1.3×10^{-3}	8.8	7.6
160 °C	3.2×10^{-1}	2.5×10^{-2}	12.7	10.9	1.3×10^{-2}	2.8×10^{-3}	4.8	4.1
170 °C	3.6×10^{-1}	5.5×10^{-2}	6.5	5.6	1.5×10^{-2}	6.2×10^{-3}	2.4	2.1
180 °C	4.1×10^{-1}	1.2×10^{-1}	3.5	3.0	1.7×10^{-2}	1.2×10^{-2}	1.4	1.2
E (kJ mol^{-1})	19	110			20	117		

[a]The initial reaction rates of BDO and THF were calculated when the concentration of GBL was 10 wt %.

smaller average particle sizes caused by the introduction of Ru. The increased rate of hydrogenation for ReRu/C is consistent with its larger amount of active sites. The increase in the active sites has a positive effect on the preexponential parameter, which directly improves the reaction rate constants, thereby accelerating the rate of SA hydrogenation.[40] On the other hand, the Re−Ru interaction on the ReRu/C catalyst can significantly reduce the activation energy compared with the Re/C catalyst. According to the data in Table 2, the apparent activation energy is 40 kJ mol^{-1} for the ReRu/C catalyst and 62 kJ mol^{-1} for the Re/C catalyst. The hydrogenation of SA is much easier over ReRu/C than over Re/C as a result of the lower activation energy. The Re−Ru interaction can change the reaction route and increase the reaction rate. In addition, the apparent activation energy also reveals the influence of the temperature on the rate of reaction. According to the apparent activation energy, the influence of the temperature on SA hydrogenation is more significant over the Re/C catalyst than over the ReRu/C catalyst.

3.3.2. Kinetic Study on the Hydrogenation of GBL. On the basis of the research above, a kinetic study of the hydrogenation of GBL to BDO and THF (steps 2 and 3 in Scheme 2) was also performed. The study on the kinetics of GBL hydrogenation is useful in helping to explain the reaction mechanism in terms of kinetics. The major GBL hydrogenation products were THF and BDO (total selectivity >90%) by controlling the reaction conditions. The initial reaction rates of BDO and THF were calculated when the concentration of GBL was 10 wt %.

Figures S3 and S4 show the time course of GBL hydrogenation over Re/C and ReRu/C catalysts at different temperatures. The good fitting results were obtained by data regression, as shown in Figures S3 and S4 when the reaction orders for the generation of THF and BDO were 1 and 0, respectively. All of the fitting parameters are summarized in Table 3. It is obvious that the ReRu/C catalyst significantly promotes the transformation of GBL because the apparent reaction rate constant K and the initial reaction rate r for Re−Ru/C are much bigger than those for Re/C. This phenomenon can be ascribed to the smaller average particle size and Re−Ru interaction on the ReRu/C catalyst, which has a similar influence on the hydrogenation of SA to GBL. At a constant temperature, the values of K_{BDO}/K_{THF} and r_{BDO}/r_{THF} for the ReRu/C catalyst are always significantly higher than those for the Re/C catalyst, which indicates a promotion to the generation of BDO on the ReRu/C catalyst. Kinetic data proved that the Re−Ru interaction on the ReRu/C catalyst changed the adsorption of the active component on the surface of ReRu/C catalysts, thereby contributing to ring opening of GBL by hydrogenation to BDO instead of dehydration by hydrogenation to THF. The difference of the selectivity over various catalysts can be explained by a kinetic study, the Re−Ru interaction of which will relatively increase the generation rate of BDO over THF. This further provides proof that the ReRu/C catalyst is more beneficial to the generation of BDO than Re/C catalysts. With an increase in the temperature, the values of K_{BDO}/K_{THF} and r_{BDO}/r_{THF} for both Re−Ru/C and Re/C catalysts gradually decreased in the following order: for K_{BDO}/K_{THF}, 140 °C > 150 °C > 160 °C > 170 °C > 180 °C, and for r_{BDO}/r_{THF}, 140 °C > 150 °C > 160 °C > 170 °C > 180 °C. It can be found that the generation of THF is more favorable than the generation of BDO with higher temperature. Arrhenius plots for Re/C and ReRu/C catalysts are shown in Figure 8, and the apparent activation energies are displayed in Table 3. The value of the apparent activation energy for the generation

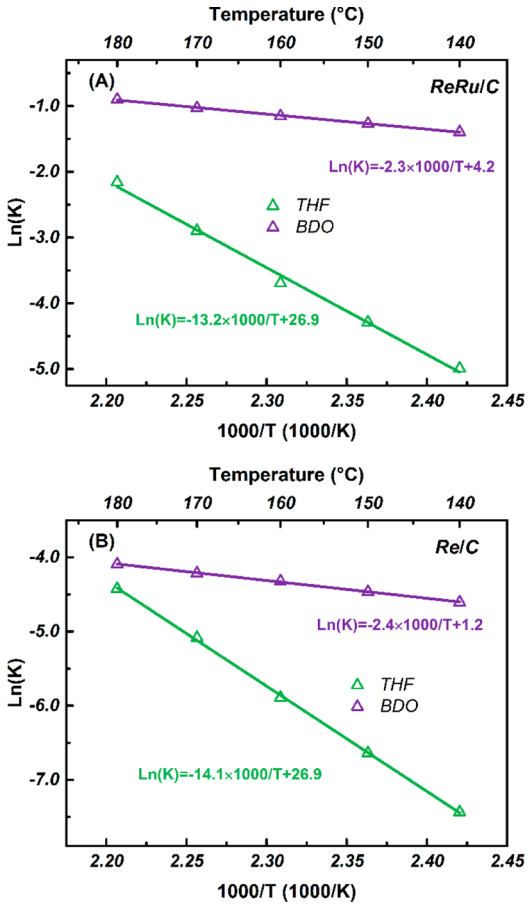

Figure 8. Arrhenius plots for the hydrogenation of GBL to THF and BDO over (A) ReRu/C (the correlation coefficient $R^2 > 0.99$) and (B) Re/C (the correlation coefficient $R^2 > 0.99$) catalysts.

DOI: 10.1021/acs.iecr.6b04875
Ind. Eng. Chem. Res. 2017, 56, 4672−4683

of THF is much higher than that for the generation of BDO over both ReRu/C and Re/C catalysts. The results show that the generation of THF is more sensitive to the temperature than the generation of BDO. Low temperature is advantageous to the ring opening of GBL, and high temperature is more advantageous to the direct hydrogenation of GBL. It is worth noting that the apparent activation energies of ReRu/C and Re/C are nearly equal on the basis of the data in Table 3. This phenomenon shows that the temperature responses of ReRu/C and Re/C catalysts for the generation of THF or BDO are very similar. The catalysts do not change the reaction route under these conditions, and the difference of the transformation rate of GBL is mainly related to the active sites.[40]

3.4. Evaluation of the Reaction Conditions. Through the above research work, the reaction conditions play a critical role in the transformation of SA. The ultimate product distribution is usually closely bonded with the catalysts and temperature. The higher apparent activation energy was observed for the generation of THF compared with the generation of BDO, according to the kinetic study. As a result, the improvement of the selectivity to BDO can benefit from the proper decrease in the temperature. On the contrary, increasing the temperature contributes to the accumulation of THF in the final products. Besides, increasing the temperature can promote the cyclodehydration of BDO to THF, which will also favor the generation of THF. Figure S5 shows the dependence of the SA concentration on the reaction time t over the ReRu/C catalyst under 180 and 220 °C. It could be found that BDO is an intermediate product and is further transformed to THF under 220 °C. The maximal relative concentration of BDO decreased from 0.47 to 0.35 and that of THF increased from 0.20 to 0.32 with an increase in the temperature. However, the hydrogenolysis of SA and its derivatives was also strengthened when the temperature was increased, manifesting that the relative concentration of NPA increased from 0.15 to 0.35. Thus, rising temperature does benefit the generation of THF, but overly high temperatures for the generation of THF were unfavored. The studies above confirm that Re−Ru bimetallic catalysts, in fact, restrain the generation of THF considering the fact that the introduction of Ru is more advantageous to generating BDO and the Ru composition also contributes to the hydrogenolysis of BDO rather than cyclodehydration. Our previous work has shown that high selectivity to THF can be obtained over a Re/C monometallic catalyst accompanied by fewer byproducts.[24] Compared with the Re monometallic catalyst, the advantage of the Re−Ru bimetallic catalyst is the improvement of the catalytic activity. The catalytic activity of the Re/C catalyst will be significantly increased when less Ru composition is introduced into it. Taking into account the balance between the catalytic activity and selectivity, THF can be produced with a Re−Ru/C bimetallic catalyst possessing a high amount of Re. From the data in Table 4, 60% selectivity to THF can be achieved over the Re3Ru/C catalyst. On the contrary, Re−Ru/C bimetallic catalysts lead to a significant improvement in the generation of BDO because of the intermetallic interaction. Low temperature is helpful not only in generating BDO but also in restraining the accumulation of byproducts. The influence of the reaction temperature on the catalytic activity should not be ignored when we consider its influence on the selectivity. Thus, excessively low temperature is inappropriate. On that basis, the experiment was performed over the ReRu/C catalyst at 160 °C and 70.1% selectivity to BDO was obtained. Compared with some other works,[16−19,22]

Table 4. Hydrogenation of SA over Re−Ru/C Bimetallic Catalysts[a]

			selectivity (%)				
catalyst	temp (°C)	concn SA (%)	GBL	BDO	THF	NBA	NPA
ReRu/C	160	99	5.7	70.1	6.5	8.9	8.8
Re3Ru/C	240	99	5.2	3.4	60.0	7.1	24.3

[a]Reaction conditions: 8.0 MPa H_2, 20 g of solutions (5 wt % SA), 0.2 g of catalysts, 10 h.

these selectivities are very competitive and the reaction conditions (temperature, H_2 pressure, reaction time, etc.) are mild in our experiments.

3.5. Stability of the Bimetallic Catalyst. The recyclability for the hydrogenation of SA over the ReRu/C catalyst was performed in our experiment by recycling four times to investigate the reusability of the catalysts. A little reaction liquid was left to protect catalysts from oxidation, and most of it was separated by centrifugation after the reaction. Then, the reaction was performed by using the catalysts left and a fresh reaction medium. Figure S6 shows the results for the aqueous hydrogenation of SA over ReRu/C catalysts with respect to the recycle run. After four cycles, a slight drop of the catalytic activity was detected in our experiment. Through analysis by ICP-AES for the reactant solution, no significant leaching of Re or Ru was detected from the catalysts. The research on the reusability of the ReRu/C catalyst indicates that the ReRu/C catalysts prepared with the MAT method, which relies on the thermolytic effect of microwave irradiation, are stable in the aqueous hydrogenation of SA.

Nowadays, SA can be obtained from the fermentation of biowastes. Optimization of the fermentation process for SA production is currently underway. To that end, various natural succinate-producing strains of bacteria and engineered *Escherichia coli* strains have been investigated. Some impurities such as acetic acid and pyruvic acid are involved in fermentation broth.[41] Therefore, it is meaningful to investigate the influence of these impurities on the catalytic activity. In these experiments, the hydrogenation reaction of SA was performed after the appropriate acetic acid or pyruvic acid were added into the reactive system, and the results are listed in Table S4. The results showed that the catalytic activity decreased to different degrees by the addition of acetic acid and pyruvic acid. We attribute the decrease in the catalytic activity to the competitive effect of acetic acid or pyruvic acid with SA. The active sites on the surface of the ReRu/C catalyst are occupied not only by SA but also by acetic acid or pyruvic acid, and the two additives will be further transformed. According to our research, acetic acid will be hydrogenated to ethanol, while the main products are 1,2-propanediol and *n*-propanol for the hydrogenation of pyruvic acid. SA continues to be transported to the desired products by the ReRu/C catalyst after the complete transformation of acetic acid or pyruvic acid, and the selectivity is not significantly influenced when the amount of impurities is 1 wt %. Besides acetic acid and pyruvic acid, formic acid (FA) is often produced, accompanied by the formation of biowastes.[42] What is interesting is that FA can be used as an attractive source of H_2 because of its cost-effectiveness and safety.[43] Therefore, the ReRu/C catalyst was used for the in situ generation of H_2 in the system by the selective decomposition of FA in an aqueous solution. The hydrogenation of SA was performed in a 1:4 aqueous mixture of SA and FA without

DOI: 10.1021/acs.iecr.6b04875
Ind. Eng. Chem. Res. 2017, 56, 4672−4683

external H_2. The results showed that the conversion of SA was very low (<5%), which is closely related to deactivation of the ReRu/C catalyst. As we all know, FA can be catalytically decomposed to CO_2 and H_2 or H_2O and CO, which leads to deactivation of the catalysts. To confirm this, the experiment of the catalytic decomposition of FA was performed under 50 °C over the ReRu/C catalyst. A large amount of gas was generated at first, and soon the reaction almost entirely stopped. It can be found that the gas products from the decomposition of FA consist of quite a lot of CO. CO occupies the active sites on the surface of the catalysts immediately and leads to deactivation; hence, one can see that FA is detrimental to this system. However, the proper amount of acetic acid or pyruvic acid is tolerable in this system.

4. CONCLUSIONS

The introduction of Ru decreases the average particle sizes of Re−Ru/C bimetallic catalysts, which exhibit good dispersion and structural properties when the catalyst was prepared with the MAT method. Because of the influence of the particle size and strong Re−Ru interaction, the ReRu/C catalyst shows maximum TOFs for the hydrogenation of SA. According to our research, the Ru composition contributes to the hydrogenolysis of carboxyl, while the Re composition is beneficial to the hydrogenation of carboxyl, and this phenomenon can be related to the nature of the active metal and the strength of adsorbed H_2. Further research on kinetics shows that apparent reaction orders of 0.6 and 1.0 for the SA concentration are observed over ReRu/C and Re/C, respectively, while the apparent reaction order is 1.9 for H_2 pressure over the ReRu/C catalyst. This indicates that the hydrogenation of SA is sensitive to the H_2 pressure and the saturability of the hydrogenation intermediates over Re/C is lower than that over ReRu/C. The Re−Ru interaction changed the adsorption and activation of the active component on the surface of Re−Ru/C catalysts, thereby contributing to ring opening of GBL by hydrogenation to BDO instead of dehydration by hydrogenation to THF over the Re/C catalyst. The kinetic study of hydrogenation of GBL also confirms that the Re−Ru interaction will relatively increase the generation rate of BDO more than that of THF. Besides, low temperature is advantageous to the ring opening of GBL and high temperature is more advantageous to the direct hydrogenation of GBL because of the fact that the value of the apparent activation energy for the generation of THF is much higher than that for the generation of BDO over both ReRu/C and Re/C catalysts. The selectivity to THF or BDO can be controlled to achieve 60% and 70%, respectively, under complete conversion according to the studies of the reaction mechanism.

■ ASSOCIATED CONTENT

Supporting Information

The Supporting Information is available free of charge on the ACS Publications website at DOI: 10.1021/acs.iecr.6b04875.

Specific information about the characterization method, scheme of the MAT method, details about the kinetic study, XRD, XPS, and H_2-TPD analysis results, hydrogenation of intermediates over Re−Ru/C bimetallic catalysts, influence of impurities on the catalytic activity and the recycle stability of Re−Ru/C, and proposed reaction mechanism of SA hydrogenation (PDF)

■ AUTHOR INFORMATION

Corresponding Author

*Tel: +86-0411-84986353. Fax: +86-0411-84986353. E-mail: changhai@dlut.edu.cn.

ORCID

Changhai Liang: 0000-0001-7959-251X

Notes

The authors declare no competing financial interest.

■ ACKNOWLEDGMENTS

We gratefully acknowledge the financial support provided by the National Natural Science Foundation of China (Grants 21573031 and 21428301), Fundamental Research Funds for the Central Universities (Grant DUT15ZD106), and Program for Excellent Talents in Dalian City (Grant 2016RD09).

■ REFERENCES

(1) Corma, A.; Iborra, S.; Velty, A. Chemical routes for the transformation of biomass into chemicals. *Chem. Rev.* **2007**, *107*, 2411−2502.

(2) Delhomme, C.; Weuster-Botz, D.; Kühn, F. E. Succinic acid from renewable resources as a C4 building-block chemical - a review of the catalytic possibilities in aqueous media. *Green Chem.* **2009**, *11*, 13−26.

(3) Hailes, H. C. Reaction solvent selection: the potential of water as a solvent for organic transformations. *Org. Process Res. Dev.* **2007**, *11*, 114−120.

(4) Serrano-Ruiz, J. C.; Luque, R.; Sepulveda-Escribano, A. Transformations of biomass derived platform molecules: from high added-value chemicals to fuels via aqueous-phase processing. *Chem. Soc. Rev.* **2011**, *40*, 5266−5281.

(5) Cukalovic, A.; Stevens, C. V. Feasibility of production methods for succinic acid derivatives: a marriage of renewable resources and chemical technology. *Biofuels, Bioprod. Biorefin.* **2008**, *2*, 505−529.

(6) Patel, M.; Crank, M.; Dornburg, V.; Hermann, B.; Roes, L.; Hüsing, B.; Overbeek, L.; Terragni, F.; Recchia, E. Medium and long-term opportunities and risks of the biotechnological production of bulk chemicals from renewable resources. *BREW Project*, 2006.

(7) Herrmann, U.; Emig, G. Liquid phase hydrogenation of maleic anhydride to 1,4-butanediol in a packed bubble column reactor. *Ind. Eng. Chem. Res.* **1998**, *37*, 759−769.

(8) Budge, J. R.; Attig, T. G. Catalysts for the hydrogenation of maleic acid to 1,4-butanediol. U.S. Patent 5,969,164, 1999.

(9) Werpy, T.; Frye, J. G.; Wang, Y.; Zacher, H. Textured catalysts, method of making textured catalysts and method of catalyzing reactions conducted in hydrothermal conditions. U.S. Patent 6,670,300, 2003.

(10) Hong, U. G.; Kim, J. K.; Lee, J.; Lee, J. K.; Song, J. H.; Yi, J.; Song, I. K. Hydrogenation of succinic acid to tetrahydrofuran over ruthenium-carbon composite catalysts: Effect of HCl concentration in the preparation of the catalysts. *J. Ind. Eng. Chem.* **2014**, *20*, 3834−3840.

(11) Corbel-Demailly, L.; Ly, B. K.; Minh, D. P.; Tapin, B.; Especel, C.; Epron, F.; Cabiac, A.; Guillon, E.; Besson, M.; Pinel, C. Heterogeneous catalytic hydrogenation of bio-based levulinic and succinic acids in aqueous solutions. *ChemSusChem* **2013**, *6*, 2388−2395.

(12) Hong, U. G.; Park, H. W.; Lee, J.; Hwang, S.; Yi, J.; Song, I. K. Hydrogenation of succinic acid to tetrahydrofuran over rhenium catalyst supported on H_2SO_4-treated mesoporous carbon. *Appl. Catal., A* **2012**, *415*−*416*, 141−148.

(13) Hong, U. G.; Kim, J. K.; Lee, J.; Lee, J. K.; Song, J. H.; Yi, J.; Song, I. K. Hydrogenation of succinic acid to tetrahydrofuran over ruthenium−carbon composite catalyst. *Appl. Catal., A* **2014**, *469*, 466−471.

DOI: 10.1021/acs.iecr.6b04875
Ind. Eng. Chem. Res. 2017, 56, 4672−4683

(14) Tapin, B.; Epron, F.; Especel, C.; Ly, B. K.; Pinel, C.; Besson, M. Study of monometallic Pd/TiO_2 catalysts for the hydrogenation of succinic acid in aqueous phase. *ACS Catal.* **2013**, *3*, 2327−2335.
(15) Chung, S. H.; Park, Y. M.; Kim, M. S.; Lee, K. Y. The effect of textural properties on the hydrogenation of succinic acid using palladium incorporated mesoporous supports. *Catal. Today* **2012**, *185*, 205−210.
(16) Minh, D. P.; Besson, M.; Pinel, C.; Fuertes, P.; Petitjean, C. Aqueous-phase hydrogenation of biomass-based succinic acid to 1,4-butanediol over supported bimetallic catalysts. *Top. Catal.* **2010**, *53*, 1270−1273.
(17) Ly, B. K.; Minh, D. P.; Pinel, C.; Besson, M.; Tapin, B.; Epron, F.; Especel, C. Effect of addition mode of Re in bimetallic Pd−Re/TiO_2 catalysts upon the selective aqueous-phase hydrogenation of succinic acid to 1,4-butanediol. *Top. Catal.* **2012**, *55*, 466−473.
(18) Kang, K. H.; Hong, U. G.; Bang, Y.; Choi, J. H.; Kim, J. K.; Lee, J. K.; Han, S. J.; Song, I. K. Hydrogenation of succinic acid to 1,4-butanediol over Re−Ru bimetallic catalysts supported on mesoporous carbon. *Appl. Catal., A* **2015**, *490*, 153−162.
(19) Ly, B. K.; Tapin, B.; Aouine, M.; Delichere, P.; Epron, F.; Pinel, C.; Especel, C.; Besson, M. Insights into the oxidation state and location of rhenium in Re-Pd/TiO_2 catalysts for aqueous-phase selective hydrogenation of succinic acid to 1,4-butanediol as a function of palladium and rhenium deposition methods. *ChemCatChem* **2015**, *7*, 2161−2178.
(20) Shao, Z. F.; Li, C.; Di, X.; Xiao, Z. H.; Liang, C. H. Aqueous-phase hydrogenation of succinic acid to γ-butyrolactone and tetrahydrofuran over Pd/C, Re/C, and Pd−Re/C Catalysts. *Ind. Eng. Chem. Res.* **2014**, *53*, 9638−9645.
(21) Deshpande, R. M.; Buwa, V. V.; Rode, C. V.; Chaudhari, R. V.; Mills, P. L. Tailoring of activity and selectivity using bimetallic catalyst in hydrogenation of succinic acid. *Catal. Commun.* **2002**, *3*, 269−274.
(22) Takeda, Y.; Tamura, M.; Nakagawa, Y.; Okumura, K.; Tomishige, K. Hydrogenation of dicarboxylic acids to diols over Re−Pd catalysts. *Catal. Sci. Technol.* **2016**, *6*, 5668−5683.
(23) Ryashentseva, M. A. Rhenium-containing catalysts in reactions of organic compounds. *Russ. Chem. Rev.* **1998**, *67*, 157−177.
(24) Di, X.; Shao, Z. F.; Li, C.; Li, W. Z.; Liang, C. H. Hydrogenation of succinic acid over supported rhenium catalysts prepared by the microwave-assisted thermolytic method. *Catal. Sci. Technol.* **2015**, *5*, 2441−2448.
(25) Kitchen, H. J.; Vallance, S. R.; Kennedy, J. L.; Tapia-Ruiz, N.; Carassiti, L.; Harrison, A.; Whittaker, A. G.; Drysdale, T. D.; Kingman, S. W.; Gregory, D. H. Modern microwave methods in solid-state inorganic materials chemistry: from fundamentals to manufacturing. *Chem. Rev.* **2014**, *114*, 1170−1206.
(26) Ni, X. J.; Zhang, B. S.; Li, C.; Pang, M.; Su, D. S.; Williams, C. T.; Liang, C. H. Microwave-assisted green synthesis of uniform Ru nanoparticles supported on non-functional carbon nanotubes for cinnamaldehyde hydrogenation. *Catal. Commun.* **2012**, *24*, 65−69.
(27) Gawande, M. B.; Shelke, S. N.; Zboril, R.; Varma, R. S. Microwave-assisted chemistry: synthetic applications for rapid assembly of nanomaterials and organics. *Acc. Chem. Res.* **2014**, *47*, 1338−1348.
(28) Baranowska, K.; Okal, J.; Miniajluk, N. Effect of rhenium on ruthenium dispersion in the Ru−Re/γ-Al_2O_3 Catalysts. *Catal. Lett.* **2014**, *144*, 447−459.
(29) Bare, S. R.; Kelly, S. D.; Vila, F. D.; Boldingh, E.; Karapetrova, E.; Kas, J.; Mickelson, G. E.; Modica, F. S.; Yang, N.; Rehr, J. J. Experimental (XAS, STEM, TPR, and XPS) and theoretical (DFT) characterization of supported rhenium catalysts. *J. Phys. Chem. C* **2011**, *115*, 5740−5755.
(30) Chary, K.; Srikanth, C.; Venkatrao, V. Characterization and reactivity of Nb_2O_5 supported Ru catalysts. *Catal. Commun.* **2009**, *10*, 459−463.
(31) Wettstein, S. G.; Bond, J. Q.; Alonso, D. M.; Pham, H. N.; Datye, A. K.; Dumesic, J. A. RuSn bimetallic catalysts for selective hydrogenation of levulinic acid to γ-valerolactone. *Appl. Catal., B* **2012**, *117−118*, 321−329.
(32) Okal, J.; Tylus, W.; Kepinski, L. XPS study of oxidation of rhenium metal on γ-Al_2O_3 support. *J. Catal.* **2004**, *225*, 498−509.
(33) Takeda, Y.; Tamura, M.; Nakagawa, Y.; Okumura, K.; Tomishige, K. Characterization of Re−Pd/SiO_2 catalysts for hydrogenation of stearic acid. *ACS Catal.* **2015**, *5*, 7034−7047.
(34) Chakroune, N.; Viau, G.; Ammar, S.; Poul, L.; Veautier, D.; Chehimi, M. M.; Mangeney, C.; Villain, F.; Fiévet, F. Acetate- and thiol-capped monodisperse ruthenium nanoparticles: XPS, XAS, and HRTEM studies. *Langmuir* **2005**, *21*, 6788−6796.
(35) Maris, E.; Davis, R. Hydrogenolysis of glycerol over carbon-supported Ru and Pt catalysts. *J. Catal.* **2007**, *249*, 328−337.
(36) Sun, J.; Liu, H. Selective hydrogenolysis of biomass-derived xylitol to ethylene glycol and propylene glycol on supported Ru catalysts. *Green Chem.* **2011**, *13*, 135−142.
(37) Rachmady, W.; Vannice, M. A. Acetic acid hydrogenation over supported platinum catalysts. *J. Catal.* **2000**, *192*, 322−334.
(38) Abdelrahman, O. A.; Heyden, A.; Bond, J. Q. Analysis of kinetics and reaction pathways in the aqueous-phase hydrogenation of levulinic acid to form γ-valerolactone over Ru/C. *ACS Catal.* **2014**, *4*, 1171−1181.
(39) Fabre, L.; Gallezot, P.; Perrard, A. Catalytic hydrogenation of arabinonic acid and lactones to arabitol. *J. Catal.* **2002**, *208*, 247−254.
(40) Xie, X.; Li, Y.; Liu, Z. Q.; Haruta, M.; Shen, W. Low-temperature oxidation of CO catalysed by Co_3O_4 nanorods. *Nature* **2009**, *458*, 746−749.
(41) McKinlay, J. B.; Vieille, C.; Zeikus, J. G. Prospects for a bio-based succinate industry. *Appl. Microbiol. Biotechnol.* **2007**, *76*, 727−740.
(42) Zeikus, J. G.; Jain, M. K.; Elankovan, P. Biotechnology of succinic production and markets for derived industrial products. *Appl. Microbiol. Biotechnol.* **1999**, *51*, 545−552.
(43) Ruppert, A. M.; Jędrzejczyk, M.; Sneka-Płatek, O.; Keller, N.; Dumon, A. S.; Michel, C.; Sautet, P.; Grams, J. Ru catalysts for levulinic acid hydrogenation with formic acid as a hydrogen source. *Green Chem.* **2016**, *18*, 2014−2028.

DOI: 10.1021/acs.iecr.6b04875
Ind. Eng. Chem. Res. 2017, 56, 4672−4683